Chapter 7

Photonic Contribution to the Glass Transition of Polymers

Nobuyuki Tanaka

Additional information is available at the end of the chapter

http://dx.doi.org/10.5772/59717

1. Introduction

The glass transition for polymers has been investigated for a long time as the mysterious physical phenomena of solid or liquid phases from the initial studies on the equation of state in pressure (P), volume (V), and temperature (T) to the recent thermal analyses with the temperature modulated differential scanning calorimeter (TMDSC) [1 – 9]. Polystyrene (PS) is one of polymers taking a leading part in the studies on the glass transition of polymers, so far showing the heat capacity jump of 28 ~ 31 J/(K mol) at the glass transition. The temperature modulation of TMDSC emerged the latent heat capacity jump at the glass transition temperature (T_g), confirming the heat capacity jump data on the basis of PVT relations for PS. Also for poly(ethylene terephthalate) (PET), the abrupt heat capacity jump at T_g was observed on TMDSC curves, being not found with the standard DSC [8]. Recently, in the advances of the studies on the photonic contribution to the glass transition of polymers, the mysterious glass transition has been reasonably understood as the quantum phenomena [10 – 16]. For frozen polymer glasses, the heat capacity jump at T_g should start from the first order hole phase transition and then the glass parts should be unfrozen accompanying with the enthalpy and entropy jumps [10]. The holes are generally neighboring with the ordered parts, which are formed as pairs during the enthalpy relaxation at temperatures below T_g. First in this chapter, for isotactic PS (iPS) and PET, the heat capacity jump at the glass transition was discussed as the discontinuous change of energy in quantum state of the photon holes, followed by unfreezing of the glass parts. IPS and PET have the benzene rings being able to cause the resonance by neighboring in the side groups or the skeletal chains, respectively. Further, the details on the heat capacity jump found for iPS were also investigated for isotactic polypropylene (iPP) with methyl groups of the same 3/1 helix structure [16]. The resonance suggests the presence of remarkable photons in holes. The dimension of them is characterized by the

geometric molecular structure, e.g., the distance between reflectors such as benzene rings, affecting to the amplitude as a wave. While for the photon holes, the constant volume heat capacity could be defined as the differential coefficient of the internal energy of holes [10 – 16]. So for iPS, PET, and iPP, in order to confirm the identity in two heat capacities of ordered parts and holes in pairs, the heat capacity jump data per molar structural unit at the glass transition were compared with that per molar photon for the holes in ordered part / hole pairs. Here it should be noted that in the ordered part / hole pairs, the molar photon used for photon holes is equivalent to the molar structural unit for ordered parts numerically.

For iPS, PET, and iPP, surely the heat capacity jump at the glass transition was due to the discontinuous change of energy in quantum state of the resonant photon holes between neighboring benzene rings, but methyl groups for iPP, followed by unfreezing of the glass parts [14 – 16]. For iPS, the substance of the helix–coil transition with the enthalpy of 16.1 kJ/mol, but being smaller than the glass transition enthalpy of 18.9 kJ/mol, was shown as the ordered part / hole pairs. For PET, the ordered part / hole pairs were like the mesophase crystals with the glassy conformational disorder of ethylene glycol parts. For iPP, the helical sequences with the enthalpy of 7.4 kJ/mol or the nodules of mesophase with the enthalpy of 12.1 kJ/mol, interchanging between ordered parts and crystals automatically, were shown as the ordered part / hole pairs, depending on the presence of the crystallization upon cooling from the melt. According to above results, it could be understood that the glass transition of polymers investigated for a long time was only the collateral unfreezing phenomena of the glass parts starting by the disappearance of ordered part / hole pairs formed during the enthalpy relaxation at temperatures below T_g.

On the other hand, for iPS and iPP, from the quantum demand of hole energy at regular temperature intervals of 120 K for iPS and 90 K for iPP, the homogeneous glasses free from ordered part / hole pairs with T_g= 240 K and 180 K have been predicted, respectively [15, 16]. T_g of them could be understood as the first order glass phase transition temperature of the homogeneous glass [17, 18]. But, as one of other quantum possibilities for these polymers, the liquids with T_g= 0 K have also been predicted. In this connection, the equilibrium melting temperature, T_m^{∞}= 450 K, for α form crystals of iPP was corresponding to 5 times the interval of 90 K. The sift of melting from α to γ form crystals between two peaks of a DSC double melting peak curve observed upon heating was discussed, relating to the formation and then disappearance of crystal / hole pairs.

2. Theoretical treatments and discussion

When the hole energy in the ordered part / hole pairs excited at the glass transition, being in equilibrium with the flow parts, is given by h^h (= $3C_v^{ph}T$), the heat capacity per molar photon for holes, C_p^{h*} (= C_p^{flow}), is given by [10 – 16] (see section **4**):

$$C_p^{h\,*}\left(=C_p^{flow}\right)=3C_p^{ph}\left(1+Td\ln J_h/dT\right) \tag{1}$$

where C_p^{flow} is the heat capacity per molar structural unit for the flow parts, being equal to C_p^x of the heat capacity per molar structural unit for the excited ordered parts [19], C_v^{ph} (= 2.701R) is the constant volume molar heat capacity for photons [20], R is the gas constant, J_h is the number of holes lost by T, and 3 is the degree of freedom for photons. When $dJ_h/dT = 0$ at T_g and the end temperature, T_l, of the glass transition, C_p^{h*} at those temperatures is given by $3C_v^{ph}$. Thus, the heat capacity jump per molar photon, ΔC_p, at the glass transition is given by:

$$\Delta C_p \left(= C_p^{h^*} - C_v^{ph}\right) = 2C_v^{ph} \left(= 44.9\ J/(K\ mol^*)\right) \tag{2}$$

In Eq. (2), ΔC_p should be due to the discontinuous energy change from a quantum ground level for photons in the holes, that is, $(1/2)h\nu$ (= h_0^h/N_A) to $(3/2)h\nu$ (= $3h_0^h/N_A$), where h is Planck constant, ν (= c/λ) is the frequency per second, c is the velocity of light, λ is the wavelength, N_A is Avogadro constant, and h_0^h is the zero– point energy per molar photon, which also is used as the energy unit bellow. The holes in the excited ordered part / hole pairs should be in dynamical equilibrium with the spatial tubes between a chain and neighboring chains in the flow parts [21]. At the glass transition, the sigmoidal mean heat capacity curve of C_p as shown in Fig. 1 is observed generally. Even in this case, the C_p for ordered parts should be equal to the C_p^h of the mean heat capacity for the holes in ordered part / hole pairs at the glass transition:

$$C_p = C_p^h = \alpha C_v^{ph} + (1 - \alpha) C_p^{ph} \tag{3}$$

where α and $1 - \alpha$ are the fractions of ordered part / hole pairs with the respective holes of C_v^{ph} and C_p^{ph} (= $3C_v^{ph}$), and C_p^{ph} is the adiabatic molar heat capacity for photons. On the other hand, the C_p for ordered parts in pairs could be divided into two components [22]:

$$C_p = \Delta C_p^x + C_p^r \tag{4}$$

under $\int_{T_g}^{T_l} C_p dT = \int_{T_g}^{T_l} \Delta C_p^x dT$ and $\int_{T_g}^{T_l} C_p^r dT = 0$,

where ΔC_p^x (= $C_p^{h*} - 3C_v^{ph}$) is the relative component heat capacity per molar structural unit for the excited ordered parts and C_p^r is the heat capacity change per molar structural unit due to the crystallization followed by the melting. At the glass transition, ΔC_p^x shows a peak against T, reflecting the size distribution of ordered parts. Fig. 1 shows the representative C_p curve composed of ΔC_p^x and C_p^r at the glass transition for polymers.

Thus, for iPS, PET, and iPP, ΔC_p (= $2C_v^{ph}$) per molar photon (mol*) was compared with the reference value of heat capacity jump, ΔC_p^{exp}, per molar structural unit (mol) [8]. The results deviated from $\Delta C_p/\Delta C_p^{exp} = 1$. Table 1 shows the comparison of ΔC_p (= $2C_v^{ph}$) with ΔC_p^{exp} for these polymers, together with h^h/h_x at T_g, where h_x is the enthalpy per molar structural unit for ordered parts [14 – 16].

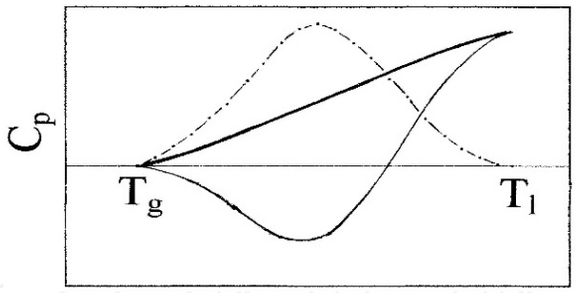

Figure 1. The components of the C_p curve (the thick line) at the glass transition for polymers. The dash – dotted line is the relative component ΔC_p^x curve for the excited ordered parts with a size distribution and the thin line is the component C_p^r curve due to the crystallization and then melting.

Polymer	T_g K	ΔC_p^{exp} J/(K mol)	ΔC_p J/(K mol*)	$\Delta C_p/\Delta C_p^{exp}$	h^h/h_x
iPS	359*1	30.8	44.9	1.5	1.5 or 1.0
PET	342	77.8 (80.4, 46.5*2)	44.9	0.6 (0.6)	1.0
iPP	270	19.2	44.9	2.3	1.5 or 2.5

The values in ( ): our data of Fig. 6. *1: see Table 2. *2: ΔC_p^{exp} at T_m^∞= 535 K.

Table 1. The values of T_g, ΔC_p^{exp}, ΔC_p (= $2C_v^{ph}$), $\Delta C_p/\Delta C_p^{exp}$, and h^h/h_x for iPS, PET, and iPP.

However, the values of $\Delta C_p/\Delta C_p^{exp}$ were correlated to h^h/h_x of the number of structural units holding one photon potentially (described below). h_x at T_g is given by [10, 23]:

$$h_x = h_g + \Delta h \tag{5}$$

where h_g {= $RT_g^2(\partial \ln v_f/\partial T)_p$} is the glass transition enthalpy per molar structural unit due to the discontinuous free volume change of v^* from $v_f = v_0$ to $v_0 + v^*$ at T_g, v_f and v_0 are the free volume and the core free volume per molar structural unit. h_g is given approximately by three expressions; (1) RT_g^2/c_2 or $\varphi_g E_a$ (in WLF equation [24], φ_g {= $1/(2.303c_1)$} is the fraction of the core free volume in glasses, c_1 and c_2 are constant, and E_a is the activation energy), (2) the molar enthalpy difference between the super – cooled liquid and the crystal at T_g; $H_g^a - H_g^c$, and (3) the sum of the conformational and cohesive enthalpies per molar structural unit at T_g; $h_g^{conf} + h_g^{int}$. For PET and iPP, the additional heat per molar structural unit, Δh, needed to melt all ordered parts by T_l in Fig. 1 is given by [10, 23]:

$$\Delta h = \Delta H - Q \tag{6}$$

where $\Delta H = H_m^a - H_c^a$, H_m^a is the enthalpy per molar structural unit for the liquid at T_m^∞, H_c^a is the enthalpy per molar structural unit for the super– cooled liquid at the onset temperature, T_c, of a DSC crystallization peak upon cooling, and Q is the heat per molar structural unit

corresponding to the total area of the DSC endothermic peak upon heating. While, in the case of $h_x^{conf} \neq h_g^{conf} = 0$ at T_g, Δh is derived as [10]:

$$\Delta h = T_g\left\{s_g^{conf} - \left(RlnZ_0\right)/x\right\} \quad (7)$$

with $s_g^{conf} = \left(RlnZ + RT_g dlnZ/dT\right)$

where h_x^{conf} is the conformational enthalpy per molar structural unit for ordered parts, s_g^{conf} is the conformational entropy per molar structural unit at T_g, Z is the conformational partition function for a chain, Z_0 (= Z/Z_t) and Z_t are the component conformational partition function for a chain regardless of temperature and depending on the temperature, respectively, and x is the degree of polymerization. For PET and iPP, the values of Δh from Eq. (7) were a little smaller than those from Eq. (6), respectively. In the case of $h_x^{conf} = h_g^{conf}$, $\Delta h = (RT_g lnZ_t)/x$ was derived, applying to nylon 6 [10].

2.1. Isotactic polystyrene

From $h^h = (3/2)N_A h\nu$ and h^h (= $3C_vT_g$) = 24.2 kJ/mol* at T_g = 359 K, the wavenumber of $1/\lambda$ = 1350 cm^{-1} was derived for a photon in holes [10]. This agreed nearly with the conformation sensitive band of 1365 cm^{-1} assigned to benzene rings [25, 26]. Further from the assigned relation of one photon to one structural unit numerically, the unity of $h^h/h_x = \Delta C_p/\Delta C_p^{exp} = 1$ at the glass transition was expected [10], applying to the ordered sequences of– *TTTT*– (see Fig. 2), where *T* is the trans isomer. However, $\Delta C_p/\Delta C_p^{exp}$ was 1.5 (see Table 1), where T_l in ΔC_p^{exp} is ~381 K [8]. Accordingly, the number of structural units holding one photon potentially in holes, n (= h^h/h_x), is defined here necessarily. Fig. 2 shows the sequence models of– *TTTT*– (n= 1) and unstable– *TCTC*– (n = 2) for iPS, where *C* is the cis isomer.

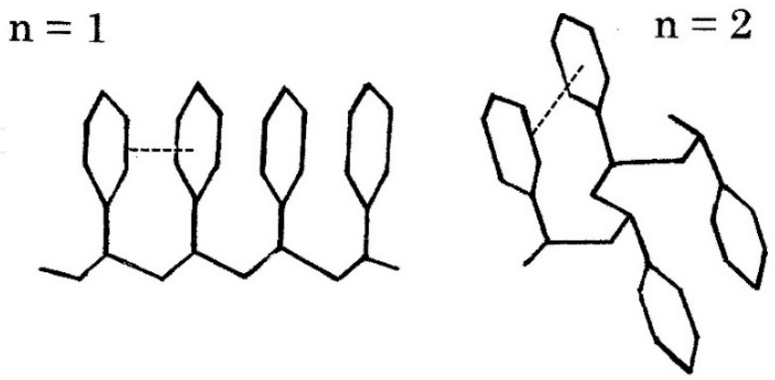

Figure 2. The sequence models of– *TTTT*– (n = 1) (Left) and unstable– *TCTC*– (n = 2) (Right) for iPS. The dashed line shows one of the photon sites between benzene rings.

According to $h^h/h_x = 1.5$, h_x (= $2h_0^h$) = 16.1 kJ/mol was derived. This corresponded to ΔC_pT_g = 16.1 kJ/mol* of the C_p jump energy for holes at T_g. While h_x can be also derived from theδ solubility parameter, δ {= $(h_0/V)^{1/2}$}, where h_0 is the latent cohesive energy per molar structural unit,

corresponding to the heat of vaporization or sublimation and V is the molar volume of structural units. The relations among h_0, h_u, h_x, and h_g at temperatures before and after T_g are given by [19, 27]:

$$h_0 = h_g + h_x \text{ or } h_g + h_x + h_u \text{ at } T \leq T_g \tag{8}$$

$$h_0 = h_x \text{ or } h_x + h_u \text{ at } T > T_g \tag{9}$$

where h_u is the heat of fusion per molar structural unit. For crystalline polymers, h_u is contained in Eqs. (8) and (9). For iPS, h_0= 35.0 kJ/mol was derived from δ = 9.16 $(cal/cm^3)^{1/2}$ of the mean of 12 experimental values (≥ 9.0 $(cal/cm^3)^{1/2}$) [28], and the value of h_x from Eq. (8), 16.1 kJ/mol, agreed with that from h^h/h_x= 1.5 perfectly. However it was smaller than h_g (= RT_g^2/c_2) = 18.9 kJ/mol. The difference in h_g and h_x, 2.8 kJ/mol, agreed with the cohesive energy of methylene residues of h_m^{int}= 2.8 kJ/mol [29], suggesting that the ordered part / hole pairs might fill softly the parts in glassy bulks.

Tg K	h_0 kJ/mol	h_g kJ/mol	Δh kJ/mol	h_x kJ/mol	h^h kJ/mol*	h^h/h_x
359*1 (360)	43.1*2	18.9	5.3	24.2*4	24.2	1
359*1 (360)	35.0*2,*3	18.9	–2.8	16.1	24.2	1.5
240	1.7*2	1.7*5	–1.7	0	0 (16.1)	---

*1: experimental value [30]. *2: from Eq. (8). *3: from δ = 9.16 $(cal/cm^3)^{1/2}$. *4: h_x for the excited ordered parts or – *TTTT*– sequences. *5: $h_g = h_g^{int} + h_g^{conf}$ from $h_g^{int} = -f_g^{conf}$ at T_g= 240 K (see Fig. 4, described below). The value in ( ) of h^h column is h^h (= $3C_v^{ph}T$) at 240 K.

Table 2. The values of T_g, h_0, h_g, Δh, h_x, h^h, and h^h/h_x for iPS.

Table 2 shows the values of T_g, h_0, h_g, Δh, h_x, and h^h at h^h/h_x= 1 and 1.5 for iPS. In the 4th line, $h^h = h_x = 0$ and h_g= 1.7 kJ/mol at 240 K are shown (discussed below). The relation of $h^h = h_x = 0$ is brought by the energy radiation of $2h_0^h$ (= 16.1 kJ/mol*) at T_g and the energy loss of h_0^h (= 8.1 kJ/mol*) upon cooling from T_g obeying:

$$h^h = h_0^h - 3C_v^{ph}\left(T_g - T\right) \tag{10}$$

In Eq. (10), the specific temperature of 240 K at h^h= 0 agreed with the hole temperature at h^h (= $3C_v^{ph}T$)= 16.1 kJ/mol*. In the glasses upon heating from 0 K, the generation of ordered part / hole pairs at 240 K and succeedingly, the instant radiation of the hole energy of 16.1 kJ/mol* should bring the same state as that of h^h= 0 at 240 K upon cooling, suggesting T_g= 240 K for the homogeneous glass free from the ordered part / hole pairs. Altering $3C_v^{ph}$ (= C_p^{ph}) in Eq. (10) to C_v^{ph}, the temperature at h^h= 0 was T_g= 0 K. While for the glasses including the ordered part /

hole pairs, T_g= 360 K (see Table 2) was expected from the quantum demand of hole energy at regular temperature intervals of 120 K.

For iPS, the rotational isomeric 2–state (RIS) model of *T* (trans) and *G* (gauche) or *G′* (gauche′) is known well [31]. Fig. 3 depicts the helix structure of – *TGTGTG* – (n = 3) for iPS. From h^h/h_x (= n) = 1.5, the intermediate sequences (n = 1.5) between the right or left handed helical sequence (n = 3) and the aperiodic sequence (n = 0), displaying the helix–coil transition, were predicted as the sequences of ordered parts [14, 15]. The frequency of occurrence, Γ, of the helix–coil transition should be given approximately by $h^h/h_0{}^h$ in Eq. (10) with $h^h/h_0{}^h$= 0 at T = 240 K. The ΔC_p (= $3C_v{}^{ph}$) at T_g= 240 K in a glassy state of Γ = 0 was 67.4 J/(K mol*) [15].

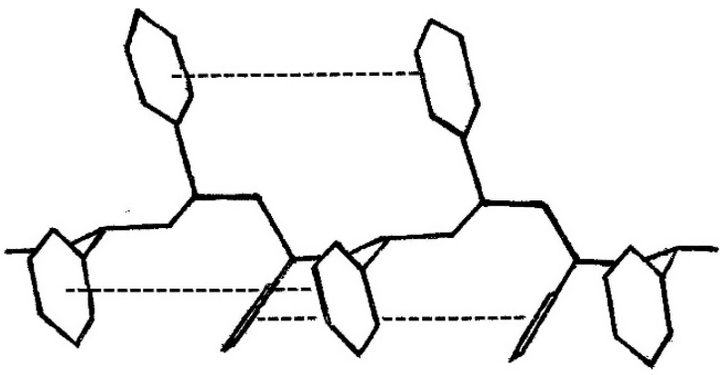

Figure 3. The 3/1 helix structure of – *TGTGTG*– (n = 3) and the photon sites (dashed line parts) between benzene rings for iPS.

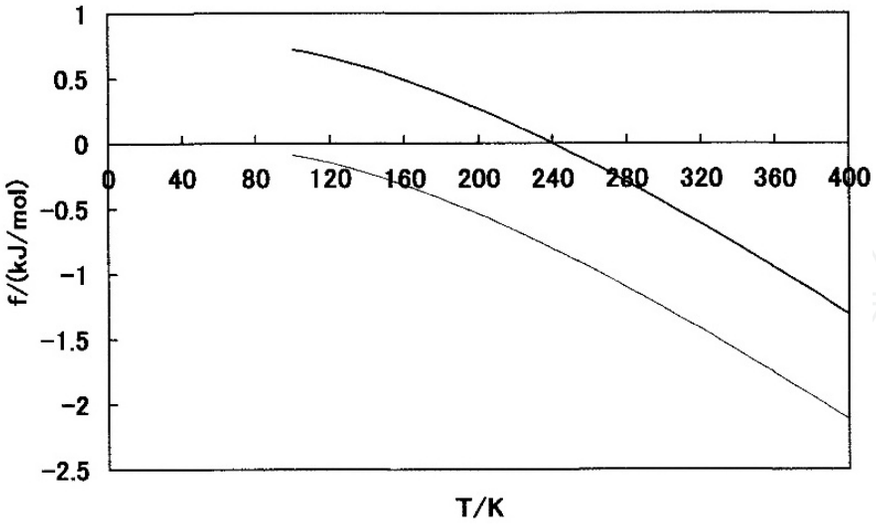

Figure 4. The relation between f and T calculated for the RIS model chains (x = 100) of iPS. The thin line is $f = f^{conf}$ and the thick line is $f = f^{conf}$+ 0.81 kJ/mol.

Fig. 4 shows the relation between f (= f^{conf} or f^{conf}+ 0.81 kJ/mol) and T calculated for the RIS model chains (x = 100) with the normalized statistical weight of η = 1 applied to *TG* isomer of

iPS, where f^{conf} is the conformational free energy per molar structural unit, being minus and decreasing with an increase in temperature. Adding the value of $-f^{conf}$ (= 0.81 kJ/mol) at 240 K to all values of the original thin line, the thick line of f^{conf}+ 0.81 kJ/mol is depicted. In the case of $-f^{conf} = h^{int}$, i.e., $(h^{conf} + h^{int}) - Ts^{conf} = 0$ at 240 K, the sum of $-f^{conf}$ (= 0.81 kJ/mol) and h^{conf} (= 0.89 kJ/mol), 1.70 kJ/mol, should be the ultimate h_g at the first order glass phase transition for the homogeneous glass free from the ordered part / hole pairs (see Table 2), where h^{int} is the cohesive enthalpy per molar structural unit, and h^{conf} and s^{conf} are the conformational enthalpy and entropy per molar structural unit.

Fig. 5 shows the schematic chart of the instantaneous state changes at T_g (= 360 K) upon cooling and heating as a working hyposesis. The ordered part / hole pairs formed instantaneously at T_g upon cooling have $h^h = h_0^h$ and $h_x = 2h_0^h$. At T_g upon heating, the ordered part / hole pairs are excited by absorbing the photon energy of $2h_0^h$ for the holes and adding the energy of h_0^h for the ordered parts, followed by the absorption of h_g for the glass parts. The equilibrium relation at the melting transition among the ordered parts, the holes, and the flow parts is shown by the dashed lines in Fig. 5. In order to melt the excited ordered part / hole pairs perfectly, further the latent heat of h_0^h is needed at T_g.

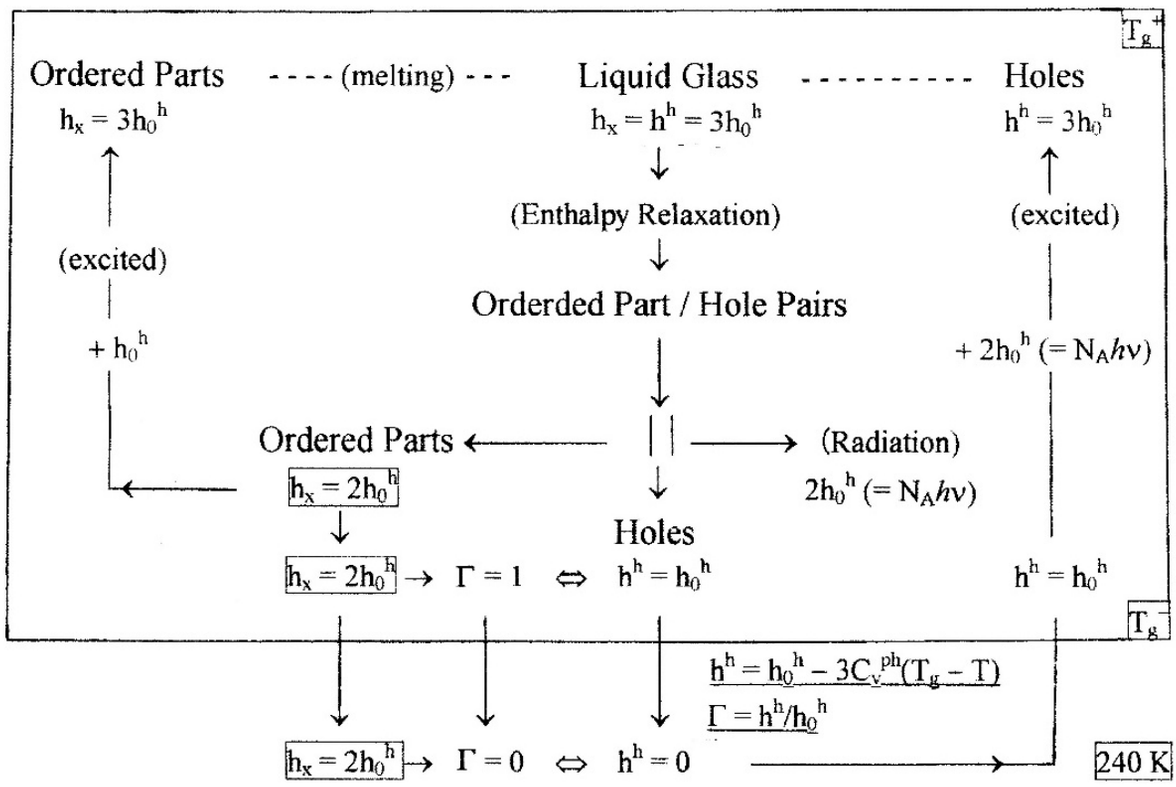

Figure 5. The schematic chart of the instantaneous state changes at T_g for iPS. The arrow marks of ↓ and ↑ show the cooling and heating directions, respectively. T_g^+ and T_g^- are the glass transition temperatures upon cooling and heating, respectively. The $h_x = 2h_0^h$ shows the substance of helix–coil transition between the helical sequence (n = 3) and the aperiodic sequence (n = 0). The arrow marks of ⇔ show the interaction between the ordered parts and the holes in the pairs. The Γ is the frequency of occurrence of the helix–coil transition. The dashed lines show the equilibrium relation of melting among ordered parts, flow parts, and holes in the excited state.

2.2. Poly(ethylene terephthalate)

For PET, h_x (= h_g+ Δh) = 24.1 kJ/mol was obtained from Eq. (5), being almost equal to h^h (= $3C_v{}^{ph}T_g$) = 23.0 kJ/mol* at T_g (= 342 K) [10, 23]. Thus, h^h/h_x (= n) = 0.95 was shown experimentally. However as shown in Table 1, $\Delta C_p/\Delta C_p{}^{exp}$ was 0.6. Table 3 shows the values of T_g, h_0, h_u, h_g, Δh, h_x, h^h, and h^h/h_x for PET. The two values of h_u, 23.0 and 28.5 kJ/mol, are assigned to the crystals with the conformational disorder of ethylene glycol parts and the smectic–c crystals with the stretched sequences, respectively [23, 32]. $\Delta C_p/\Delta C_p{}^{exp}$= 0.6 at the glass transition meant that one photon was situated in the neighboring phenylene residues comprising ~60 % of the structural unit length and 40 % of $\Delta C_p{}^{exp}$ was brought by unfreezing of the ethylene glycol parts in a glass state [14]. This was predicted also from the data by TMDSC [8]. From h^h= (3/2) $N_A h\nu$ and h^h (= $3C_v{}^{ph}T_g$) = 23.0 kJ/mol* at T_g= 342 K, $1/\lambda$ = 1290 cm^{-1} was derived, agreeing with 1288 cm^{-1} observed for the un–oriented samples [33].

T_g K	h_0 kJ/mol	h_u kJ/mol	h_g kJ/mol	Δh kJ/mol	h_x kJ/mol	h^h kJ/mol*	h^h/h_x
342	64.7*1	23.0 (535 K)	17.6*3	6.5	24.1	23.0	0.95
342	70.2*1, 68.2*2	28.5 (549 K)	17.6*3	6.5	24.1	23.0	0.95

*1: from Eq. (8). *2: from δ = 10.7 $(cal/cm^3)^{1/2}$ [19]. *3: $h_g = RT_g{}^2/c_2{}^2$. The values in () are $T_m{}^\infty$ of the respective crystals [23].

Table 3. The values of T_g, h_0, h_u, h_g, Δh, h_x, h^h, and h^h/h_x for PET.

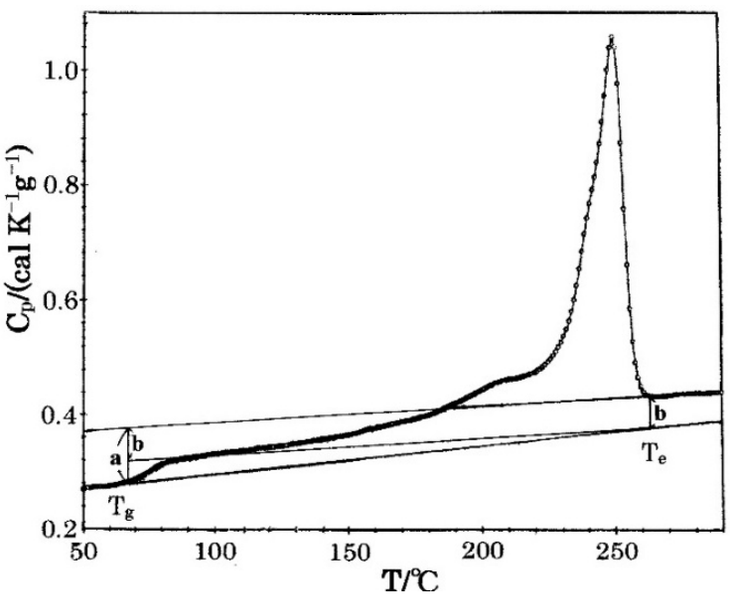

Figure 6. The C_p curve for the non–annealed PET film. The parts of a and b show the C_p jump to the liquid line at T_g and T_e.

Fig. 6 shows the C_p curve converted from DSC curve data for the non–annealed PET film cooled to 323 K (50 °C) at 5 K/min from 573 K (300 °C). T_g agreed almost with 342 K of [8]. T_e of the

end temperature of melting is 535 K (262 °C). The parts of a, b, and a – b of C_p jump to the liquid line at T_g and T_e were correlated to the structural unit length, the lengths of phenylene and glassy ethylene glycol residues, respectively. Fig. 7 shows the parts in the structural unit related to a, b, and a – b.

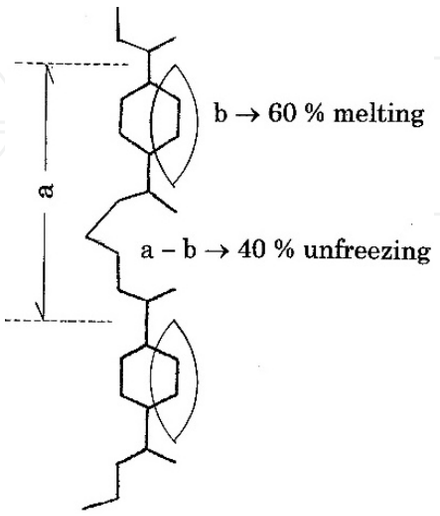

Figure 7. The parts in the structural unit related to the C_p jumps of a, b, and a – b shown in Fig. 6 for PET. The part attached to the spindle mark shows the phenylene residue holding one photon together with the neighboring same residue (omitted here).

2.3. Isotactic polypropylene

According to the scheme of the formation of ordered part / hole pairs at T_g upon cooling (see Fig. 5), for iPP with T_g= 270 K, h_x (= $2h_0^h$) = 12.1 kJ/mol was derived, being much larger than $h_g \approx H_g^a - H_g^c$= 6.2 kJ/mol [34] and h_x (= h_g+ Δh) = 7.4 kJ/mol, where Δh = ΔH – Q, ΔH = $H_m^a - H_c^a$ (see Eqs. (5) and (6)). The used data are as follows: T_c= 403.6 K, T_m^∞= 450 K for α form crystals, ΔH = 4.89 kJ/mol [34], and Q = 3.76 kJ/mol for the sample annealed at 461.0 K for 1 hour [10, 35]. However, h_0 (= h_g+ h_x) = 18.3 kJ/mol from Eq. (8) was almost equal to h^h (= $3h_0^h$) = 18.2 kJ/mol*, meaning the appearance of frozen glasses with h_g= h_0^h+ 0.1 kJ/mol. For holes with C_p^{ph} even upon cooling from T_g, Eq. (10) showed the specific temperature of 180 K, at which all ordered part / hole pairs should be disappeared because of h^h= 0, corresponding to 240 K for iPS [15]. At temperatures below 180 K, all should be in a state of the homogeneous glass with T_g= 180 K. The ΔC_p (= $3C_v^{ph}$) = 67.4 J/(K mol*) at T_g= 180 K was the same as that of iPS with T_g= 240 K. Fig. 8 shows the relation between f (= f^{conf} or f^{conf}+ 0.1 kJ/mol) and T calculated for RIS model chains (x = 100) with the normalized statistical weight of σ = 1 applied to *TT* isomer of iPP [36, 37]. The f^{conf} at temperatures below and above 180 K is minus and decreases with an increase in temperature. The absolute value of f^{conf}= – 0.102 kJ/mol at 180 K equaled to $h_g - h_0^h$= 0.1 kJ/mol at 270 K. Adding the cohesive enthalpy of h^{int}= 0.102 kJ/mol to f^{conf} (= – 0.102 kJ/mol), from f = f^{conf}+ h^{int}= 0 and h^{conf}= 0.18 kJ/mol at T_g= 180 K, h_g (= h^{conf}+ h^{int}) = 0.28 kJ/mol is derived as the first order glass phase transition enthalpy for the homogeneous glass composed

of isolated chains, but with the cohesive energy of h^{int} and free from ordered part / hole pairs (see Table 5).

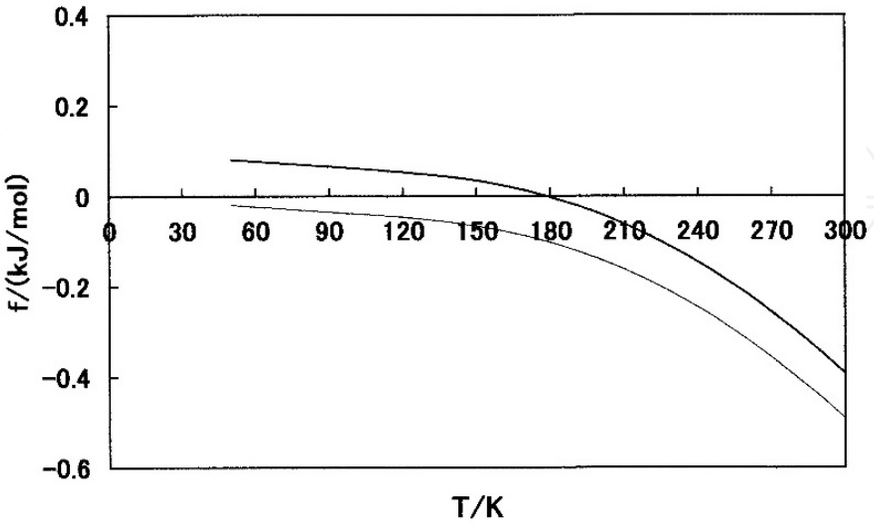

Figure 8. The relation between f and T calculated for RIS model chains (x = 100) of iPP. The thin line is $f = f^{conf}$ and the thick line is $f = f^{conf} + 0.1$ kJ/mol.

On the other hand, altering $3C_v^{ph}$ (= C_p^{ph}) in Eq. (10) to C_v^{ph}, the temperature at $h^h = 0$ was T_g= 0 K as well as iPS. From s^{conf}= 0.38 J/(K mol) of constant at temperatures below 70 K, the sequence model of – *TGTGTG**TT**G′TG′TG′T*– in a liquid state was predicted, where *T* is trans, *G* is gauche, *G′* is gauche′ isomer, and *TT* is the trans–trans isomer shifting always to the left or right direction on a sequence [38]. From h_x= 12.1 kJ/mol, the nodules of mesophase interchanging between crystals and ordered parts automatically were predicted in the glasses. According to the equilibrium relation in crystals and ordered parts of this class (D in Table 4) given by $f_x = 2f_u$ [10, 39], $2h_u - h_x$= 2.9 kJ/mol was derived using h_u= 7.5 kJ/mol for α form crystals, corresponding to $2T_m(s_u - s_x/2)$, which was almost equal to h_m^{int}= 2.8 kJ/mol of the cohesive energy of methylene residues in the sequences, where f_x and s_x are the free energy and entropy per molar structural unit for ordered parts, and f_u and s_u are those for crystals.

According to Flory's theory [40] on the melting of the fringe–type crystals with a finite crystal length of ζ, the end surface free energy of crystals per unit area, σ_e, at $(df_u/d\zeta)_\phi = 0$ is given by:

$$\sigma_e = \mu(RT\zeta/2)[1/(x - \zeta + 1) + (1/\zeta)ln\{(x - \xi + 1)/x\}] \tag{11}$$

where ϕ is the amorphous fraction and μ is the conversion coefficient of mol/m^3. In this context:

$$2\sigma_e/\zeta = \mu(f_x - f_u) \tag{12}$$

$$f_x' = RT[(1/\zeta)ln\{(x - \zeta + 1)/x\} - lnP_c] \tag{13}$$

where P_c, given by $\{(x - \zeta + 1)/x\}^{1/\zeta}$ for fringe–type crystals, is the probability that a sequence occupies the lattice sites of a crystalline sequence. Moreover:

$$f_u - \left(f_x - f_x'\right) = 0 \tag{14}$$

Eq. (11) is obtained when $\ln P_c = -1/(x - \zeta + 1)$. From Eq. (14), the relations are derived based on f_u and f_x at $f_x' \geq 0$, and those can be grouped into four equilibrium classes (A ~ D) and one non–equilibrium class (X) as shown in Table 4. Class A of $f_x = f_u$ at $f_x' = 0$ shows the dynamic equilibrium relation between the ordered parts and the crystal parts of same fringe–type, leading to $\sigma_e = 0$, and that, $\zeta = 0/0$ in Eq. (16) (described below). For class B, $f_u = -f_x'$ from Eq. (14) with $f_x = 0$ refers to the anti–crystal holes and $f_x = 0$ is assigned to the ordered parts of $\zeta = \infty$. The interface between the anti–crystal holes and the ordered parts should work as the reflector of photons. In this case, the even interface made of the folded chain segments should be avoided through the random reflection. According to Eq. (12) with $h_x - h_u = \sigma_e/(\mu\zeta)$, the respective interface energies of the hole and the ordered part are compensated each other at the common interface, thus leading to $f_x = 0$ [10]. For class C, $f_x = f_x'$ from Eq. (14) with $f_u = 0$ is assigned to the ordered parts of $\zeta \neq \infty$ (i.e., a kebab structure) and $f_u = 0$ to the crystals of $\zeta = \infty$ (i.e., a shish structure). Class D of f_u $(= f_x')$ $= f_x/2$ is related to the equilibrium in crystal and ordered parts. For those with folded chains, the reversible change from crystal or ordered parts to other parts is expected to take place automatically. The relations in class X do not satisfy Eq. (14), suggesting that the holes of class B cannot be replaced by the crystals with $\zeta \neq \infty$. Fig. 9 shows the schematic structure models of bulk polymers conformable to A ~ X classes in Table 4.

f_x'	f_x	f_u	Class
$f_x' = 0$	$f_x = f_u$	$f_u = f_x$	A
$f_x' > 0$	$f_x = 0$	$f_u = -f_x'$	B
	$f_x = f_x'$	$f_u = 0$	C
	$f_x = 2f_u$	$f_u = f_x/2 = f_x'$	D
$f_x' > 0$	$f_x = 0$	$f_u = f_x'$	X

Table 4. Relations of equilibrium (A ~ D) and non–equilibrium (X) in f_x and f_u at $f_x' \geq 0$ for crystalline polymers [10, 39].

At the rapid glass transition absorbing the photon energy of $2h_0^h$ at T_g upon heating, the ordered part / hole pairs should be excited immediately and then melted, followed by unfreezing of the glass parts. At the slow glass transition, the disappearance and then crystallization of ordered part / hole pairs should occur upon heating, bringing the new crystal parts [16]. In the closed system that the both heats of crystallization and melting should be cancelled out according to Eq. (4), those should be melted by T_l in Fig. 1. While in the open system that the heat irradiated by crystallization was escaped out of the system, T_l corresponded to T_m^∞ (450 K for α form crystals) and h_0 $(= h_g + h_x + h_u) = 21.0$ kJ/mol in Eq. (8) agreed

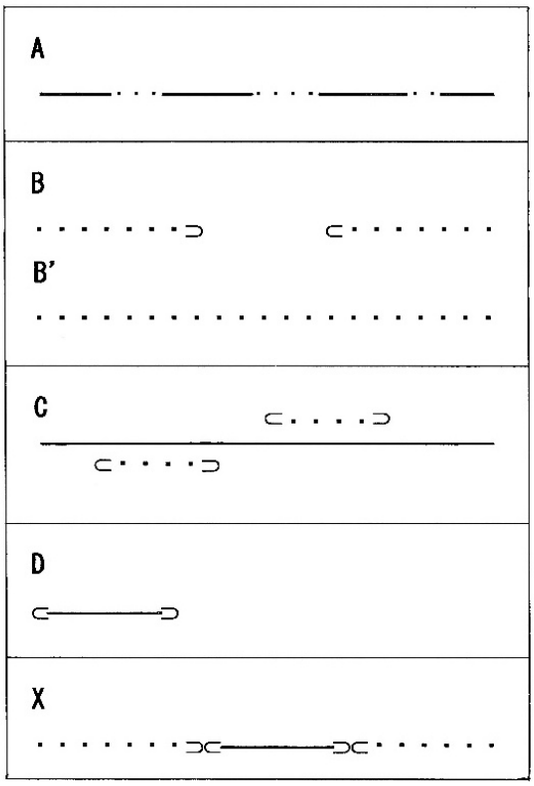

Figure 9. Schematic structure models of bulk polymers. A ~ X correspond to the classes in Table 4, respectively. •••: ordered parts, ¾¾ : crystals, ⊃ and ⊂: folded segments, the space between ⊃ and ⊂ of B: anti–crystal hole. B is equivalent to B′.

perfectly with the value of h^h (= $3h_0^h$)+ h_m^{int}, where h_x (= h_g+ Δh) is 7.4 kJ/mol, being larger than h_0^h (= $h^h/3$)= 6.1 kJ/mol*. In this context, $h_g - h_0^h$= 0.1 kJ/mol, $h_x - h_0^h$= 1.3 kJ/mol, and $h_u - h_0^h$= 1.4 kJ/mol. The sum of them was equal to h_m^{int}= 2.8 kJ/mol. Thus, n (= h^h/h_x) = 2.5 was shown, almost corresponding to $\Delta C_p/\Delta C_p^{exp}$= 2.3. Table 5 shows the values of T_g, h_0, h_u, h_g, h_x, h^h, and h^h/h_x for iPP. From h^h (= $3h_0^h$) = 18.2 kJ/mol* at T_g (= 270 K), the wavenumber of $1/\lambda$ = 1022 cm^{-1} was derived for a photon in holes [10]. This agreed nearly with 1045 cm^{-1} relating to the crystallinity [41]. Accordingly, one photon should be situated between the neighboring methyl groups in the helical sequence.

Tg K	h_0 kJ/mol	h_u kJ/mol	h_g kJ/mol	h_x kJ/mol	h^h kJ/mol*	h^h/h_x
270	18.3*1	---	6.2*3	12.1	18.2	1.5
270	21.1*1	7.5*2	6.2*3	7.4	18.2	2.5
180	0.28*1	---	0.28*4	0	0	---

*1: from Eq. (8). *2: h_u for α form crystals. *3: $h_g = H_g^a - H_g^c$, *4: $h_g = h_g^{int} + h_g^{conf}$ from $h_g^{int} = -f_g^{conf}$ at T_g= 180 K.

Table 5. The values of T_g, h_0, h_u, h_g, h_x, h^h, and h^h/h_x for iPP.

2.3.1. Equilibrium melting temperature, T_m^∞

For PET discussed in the previous section **2.2**, T_l in Fig. 1 corresponded to T_m^∞= 535 K for the crystals with conformational disorder of ethylene glycol parts, but with a chain axis parallel to c-axis of a cell. This finding in PET was also discussed in iPP with T_m^∞= 435 K, 450 K, and 462 K for β, α, and γ form crystals, respectively, which were found by DSC measurements [35]. Above all, T_m^∞= 450 K for α form crystals could be T_l (in Fig.1) of the temperature expected from the quantum demand of hole energy at regular temperature intervals of 90 K. Experimentally, T_m^∞ is determined as the intersection temperature between an extrapolation line of T_m= T_e in the melting peaks without superheating and a T_m= T_a line, where T_m is the melting temperature from T_a to T_e, T_a is the annealing (crystallization) temperature, and T_e is the end temperature of melting peak. While at T_m^∞, the processes of melting and crystallization should occur reversibly, so that T_m^∞ equals to both temperatures of T_e and T_b of the onset temperature of melting, and that, there are two points of T_m^∞ at T_a (= T_e) and T_b (= T_e) on a T_m= T_e line. The line through two points of T_m^∞ should be parallel to the abscissa of T_a, because T_m^∞ is only one [23]. For the bulk contained α form crystals with h_u= 7.46 kJ/mol, the sum of $h_g - h_0^h$= 0.1 kJ/mol, $h_x - h_0^h$= 1.3 kJ/mol, and $h_u - h_0^h$= 1.4 kJ/mol was equal to h_m^{int}= 2.8 kJ/mol (see section **2.3**). While for the bulk contained only γ form crystals with h_u= 8.70 kJ/mol, the difference in h_m^{int} and ($h_u - h_0^h$) was 0.2 kJ/mol, suggesting h_g= h_x= h_0^h+ 0.1 kJ/mol. Figs. 10 and 11 show the DSC single and double melting peak curves for the iPP films annealed at T_a= 461.0 K and 441.5 K for 1 hour, respectively. Here the single melting peak curve in Fig. 10 is divided into α and β peaks, and the double melting peak curve in Fig. 11 is divided into γ, α, and β peaks. In both Figures, T_b is the temperature that the extrapolation line from the line segment with a highest slope in the lower temperature side of the melting peak intersects the base line. The onset temperature of the extrapolation line, T*, is also the end temperature of the residual peak appeared by subtracting the area of single or double peak with T_b from the total endothermic peak area. The β peak is considered to be due to the melting of small crystals attached around the crystal lamellae of α form. The mean of end temperatures in β peaks found for some annealing samples agreed closely with T_e= 435 K of β form crystals [42].

Table 6 shows the values of T_b, T*, Q_m, ΔQ_m, Δh^h, and $\Delta h^h/\Delta Q_m$ in α and γ peak curves for the iPP films annealed at 461.0 K and 441.5 K for 1 hour. Where Q_m is the heat per molar structural unit corresponding to the area of α or γ peak from T_b and ΔQ_m is the heat per molar structural unit corresponding to the area from T_b to T* of α or γ peak and relating to the melting of crystals recrystallized newly from β to α form or α to γ form. For the holes of crystal / hole pairs formed newly by recrystallization from T_b to T* of β or α peak, the hole energy per molar photon, Δh^h, is given by [10]:

$$\Delta h^h = 3C_v^{ph}\left(T^* - T_b\right) \tag{15}$$

As shown in Table 6, the small difference in ΔQ_m and Δh^h could be regarded as significant for the formation and then disappearance of crystal / hole pairs from T_b to T*. For the shift from

http://dx.doi.org/10.5772/59717

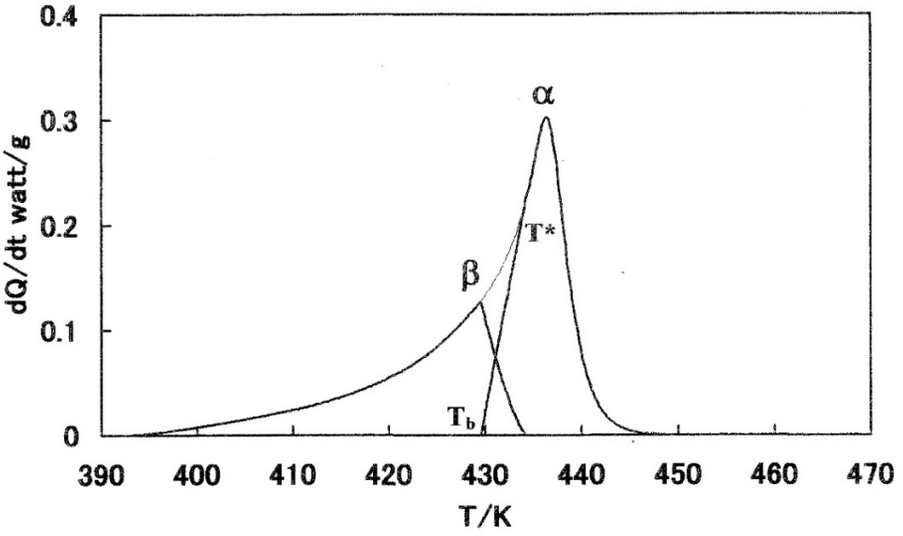

Figure 10. DSC single melting peak curve composed of α and β peaks for the iPP film annealed at 461.0 K for 1 hour. The thin line is the part of an original DSC curve. T_b is the onset temperature of α peak and T* is the end temperature of β peak.

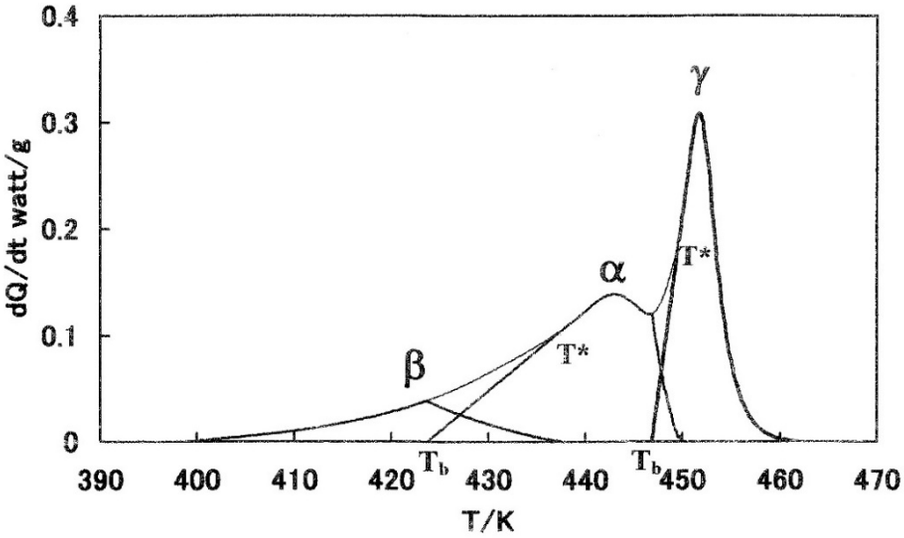

Figure 11. DSC double melting peak curve composed of α, β, and γ peaks for the iPP film annealed at 441.5 K for 1 hour. The thin lines are the parts of an original DSC curve. T_b is the onset temperature of γ or α peak and T* is the end temperature of α or β peak.

β to α peak in Fig. 11, $\Delta h^h/\Delta Q_m$ was 1.21 contrary to our expectation, but at T*= 435 K of the mean of T* (T_m^∞ for β form crystals), $\Delta h^h/\Delta Q_m$= 0.98 was derived. For the shift from α to γ peak, it was 0.61, meaning the melting of original γ form crystals with 39 % of ΔQ_m; 0.13 kJ/mol. The relay of melting from α to γ form crystals between two peaks of a DSC double melting peak curve should be done through the mediation of the formation and then disappearance of the crystal / hole pairs with 61 % of ΔQ_m; 0.20 kJ/mol (= Δh^h), which agreed with the difference in h_m^{int} and ($h_u - h_0^h$) perfectly, corresponding to ($h_g + h_x$) – $2h_0^h$= 0.2 kJ/mol suggested above.

T_a K	Form	T_b K	T* K	Q_m kJ/mol	ΔQ_m kJ/mol	Δh^h kJ/mol	$\Delta h^h/\Delta Q_m$
461.0	α	429.6	434.2	2.05	0.38	0.24	0.63
441.5	α	423.7	437.7 (435)	2.16	0.78	0.94 (0.76)	1.21 (0.98)
	γ	446.9	449.9	1.64	0.33	0.20	0.61

The values in ( ) show T_m^∞, Δh^h, and $\Delta h^h/\Delta Q_m$ at T_m^∞ for β form crystals.

Table 6. The values of T_b, T*, Q_m, ΔQ_m, Δh^h, $\Delta h^h/\Delta Q_m$ of α and γ peak curves for the iPP films annealed at 461.0 K and 441.5 K for 1 hour.

2.3.2. ζ distribution function, F (ζ)

Next, the α peak curve in Fig. 10 and the two divided peak curves of α and γ in Fig. 11 starting to melt at T_b were converted into the crystal length (ζ) distribution function, F(ζ). The ζ is according to Gibbs–Thomson given by:

$$\zeta = \{T_m^\infty / (T_m^\infty - T_m)\}\{2\sigma_e / (\mu h_u)\} \tag{16}$$

where T_m is the corrected melting temperature. In the calculation of ζ, the values of T_m^∞, h_u, h_x, σ_e, and the corrected T_m are needed previously. For h_u, the reference value was used (see Table 8). The value of σ_e was evaluated by [43, 44]:

$$\sigma_e = \mu h_u c^* [\{RT_m^2 + (H_x - h_x)(T_m^\infty - T_m)\}] / \{2(H_x - h_x)T_m^\infty\}] \tag{17}$$

with $H_x = 2h_u - Q_m$

where c* is the cell length of c–axis. The term of square blanket in Eq. (17) is dimensionless. h_u refers to the heat of fusion of crystals with a crystal form liking to evaluate σ_e. h_x could be calculated from Eqs.(5) and (6), but in Fig. 11, using $H_m{}^a$ at T_m^∞ of the other α or γ form crystals (sub–crystals). Table 7 shows the values of h_x for the iPP films annealed at 461.0 K and 441.5 K for 1 hour, together with the values of T_c, T_b, T_e, Q, ΔH, Δh, and h_g used in the calculation of h_x. Q and ΔH are defined in Eq. (6). The value of h_x for the iPP sample of T_a= 441.5 K was smaller than h_u of the sub–crystals (see Table 8). Further, the value of h_x in the row of γ form, 6.85 kJ/mol, was ~0.7 kJ/mol larger than h_g (= 6.22 kJ/mol). Also the value of h_x in the line of α form, 8.07 kJ/mol, was ~0.7 kJ/mol larger than h_x (= 7.35 kJ/mol) for the sample of T_a= 461.0 K. Therefore, the value of h_0 (= h_g+ h_x+ h_u) in Eq. (8) for the iPP sample annealed at 441.5 K was 0.7 kJ/mol larger than that for the iPP sample of T_a= 461.0 K. The cause could be attributed to Δh affected by F(ζ) (see Eq. 18) of α form crystals, leading the characteristic R–L image (see Fig. 15).

Form*1 (T_a/K)	T_c K	T_b K	T_e K	Q kJ/mol	ΔH kJ/mol	Δh kJ/mol	h_g kJ/mol	h_x kJ/mol
α (461.0)	403.6	429.6	449.2	3.76	4.89	1.13	6.22	7.35
α (441.5)	403.6	423.7	449.5	4.41	6.26 (γ) *2	1.85	6.22	8.07
γ (441.5)	403.6	446.9	461.9	4.41	5.04 (α) *2	0.63	6.22	6.85

*1: The form of main crystals liking to evaluate σ_e. *2: ΔH calculated using $H_m{}^a$ at $T_m{}^\infty$ of the sub–crystals with the form of α or γ shown in ( ).

Table 7. The values of h_x, T_c, T_b, T_e, Q, ΔH, Δh, and h_g for the iPP films annealed at 461.0 K and 441.5 K for 1 hour.

T_a K	Form	T_p K	h_u kJ/mol	h_x kJ/mol	h_0 kJ/mol	Q_m kJ/mol	σ_e J/m²
461.0	α	435.9	7.46	7.35	14.8	2.05	36.0×10^{-3} (26.7×10^{-3})
441.5	α	442.8	7.46	8.07	15.5	2.16	45.2×10^{-3} (30.8×10^{-3})
	γ	450.9	8.70	6.85	15.6	1.64	26.5×10^{-3} (22.2×10^{-3})

The values in ( ) are σ_e at $T_m{}^\infty$ (Q_m= 0).

Table 8. The values of σ_e, T_p, h_u, h_x, h_0 (= h_x+ h_u), and Q_m for the iPP films annealed at 461.0 K and 441.5 K for 1 hour.

Table 8 shows the values of σ_e at T_p for α and γ form crystals contained in the iPP films annealed at 461.0 K and 441.5 K for 1 hour, together with the values of T_p, h_u, h_x, h_0, and Q_m used in the calculation of σ_e, where T_p is the melting peak temperature. The σ_e of α form was larger than that of γ form, because according to Eq. (17), the σ_e was mainly dependent on h_x. For α and γ forms in the sample of T_a= 441.5 K, h_0 (= h_u+ h_x) at T (> T_g) of Eq. (9) was ~15.5 kJ/mol, nevertheless the values of h_u were different. T_p is corrected by 0.6 K (436.5 K → 435.9 K) for the sample of T_a= 461.0 K and 0.2 K (443.0 K → 442.8 K) for α form and 0.8 K (451.7 K → 450.9 K) for γ form in the sample of T_a= 441.5 K to the lower temperature side, according to our concept [45].

F(ζ) is defined as [23]:

$$F(\zeta)=\left(\delta Q_m / Q_m\right)/\zeta = n_\zeta / \{N_c(T_e - T_b)\} \tag{18}$$

where δQ_m (= $\zeta n_\zeta Q_m/\{N_c(T_e - T_b)\}$) is the heat change per molar structural unit per K, n_ζ is the number of crystal sequences with ζ, N_c is the number of structural units of crystals melted in the temperature range from T_b to T_e. $\delta Q_m/Q_m$ is given by:

$$\delta Q_m / Q_m = \left(dQ / dt\right) / \int_{T_b}^{T_e} (dQ / dt) dT \tag{19}$$

where dQ/dt is the heat flow rate of DSC melting curve and t is time (see Figs. 10 and 11). Figs. 12 and 13 show F(ζ) of α and γ peak curves converted from the DSC single and double melting peak curves for the iPP films annealed at 461.0 K and 441.5 K for 1 hour.

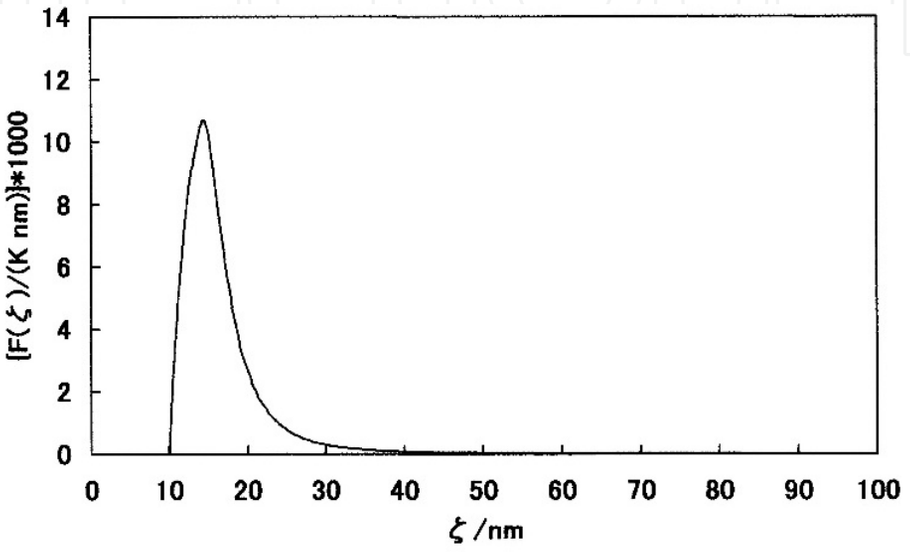

Figure 12. F(ζ) of α peak curve for the iPP film annealed at 461.0 K for 1 hour.

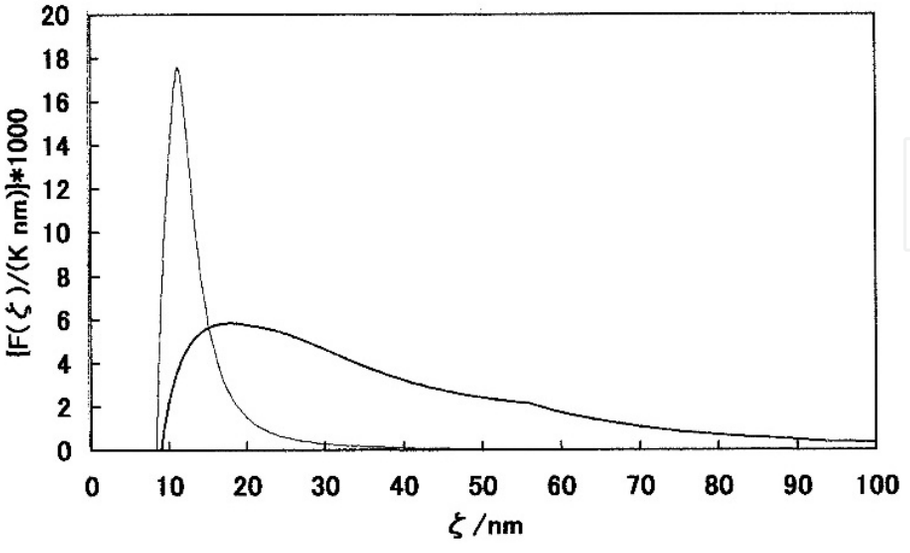

Figure 13. f(ζ) of α (thick line) and γ (thin line) peak curves for the iPP film annealed at 441.5 K for 1 hour.

Table 9 shows the ζ range and ζ_p in F(ζ) of α and γ peak curves obtained for the samples of T_a= 461.0 K and 441.5 K, where ζ_p is ζ at the maximum of F(ζ). For α peak, F(ζ) in Fig. 12 showed a sharp peak with the ζ range of 10 nm ~ 3870 nm and ζ_p= 14.6 nm, and in Fig 13, F(ζ) showed the roundish curve with the ζ range of 10 nm ~ 250 nm and ζ_p= 19.5 nm, whereas for γ peak, F(ζ) showed the sharp peak with the ζ range of 8 nm ~ 840 nm and ζ_p= 11.2 nm. The maximum of ζ was calculated using T_e (~T_m^∞) observed actually for each sample. At T_e= T_m^∞, the maximum of ζ should be infinite at $\sigma_e \neq 0$, because the melt at T_e could be interchanged in equilibrium to the imaginary crystals of ζ = ∞. In the σ_e= 0 of the class A in Table 4, ζ = 0/0 of indetermination at T_m^∞ is derived from Eq. (16). The refraction point at ζ = 55 nm on the thick line of α peak in Fig. 13 is that of dQ/dt at T_b (= 446.9 K) in Fig. 11. For the sample of T_a= 441.5 K, the ζ range of α peak was narrower than that of γ peak, because upon cooling, α form crystals should be formed around γ form crystals. As the result, the value of h_x at the interfaces between α and γ form crystals increased only ~0.7 kJ/mol (derived above). The ζ range of α peak calculated for the sample of T_a= 461.0 K was much larger than those of α and γ form crystals for the sample of T_a= 441.5 K.

T_a K	Form	ζ range nm	ζ_p nm
461.0	α	10 - 3870	14.6
441.5	α	10 - 250	19.5
	γ	8 - 840	11.2

Table 9. The ζ range and ζ_p in F(ζ) of α and γ peaks for the iPP films annealed at 461.0 K and 441.5 K for 1 hour.

In the last stage, the ζ distribution of a single–crystal like image was drawn from F(ζ). The number of crystal sequences in a radius direction, R_n, is given by [10]:

$$R_n = \left(\Delta N / \pi\right)^{1/2} \tag{20}$$

with $\Delta N = N_c\left(T_e - T_b\right)\left(\int_{\zeta_n}^{\zeta_x} F(\zeta)d\zeta - \int_{\zeta_n}^{\zeta} F(\zeta)d\zeta\right)$

where ζ_x and ζ_n are the maximum and the minimum of ζ, respectively. Figs. 14 and 15 show the representation of R (= $\pm R_n$) and L (= $\pm\zeta/2$) for α and γ form crystals in the iPP films (per 1g) annealed at 461.0 K and 441.5 K for 1 hour.

From the comparison of both figures, the change of image in α form crystal lamellae by annealing, and further in Fig. 15, the difference in packing states of α and γ form crystals in same ζ range can be seen at the view of 2D disk image.

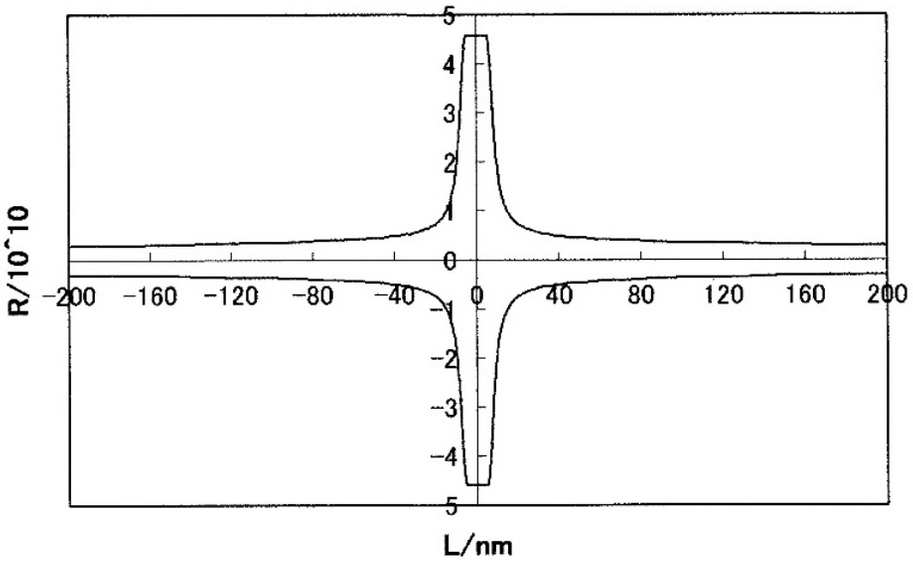

Figure 14. Representation of R (= $\pm R_n$) and L (= $\pm\zeta/2$) for α form crystals in the iPP film (per 1g) annealed at 461.0 K for 1 hour. The horizontal lines show R of the imaginary crystals melting from ζ_n to ζ= 0.

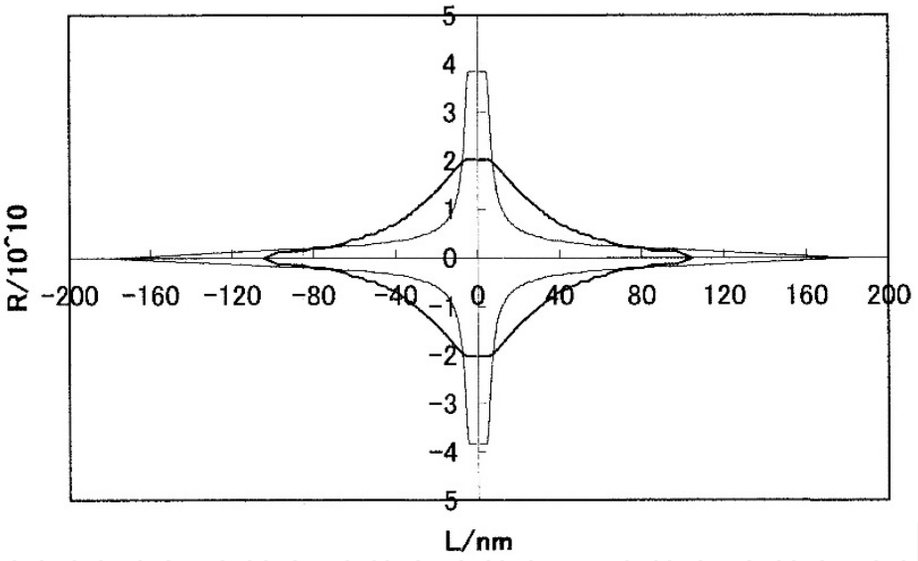

Figure 15. Representation of R (= $\pm R_n$) and L (= $\pm\zeta/2$) for α (thick line) and γ (thin line) form crystals in the iPP film (per 1g) annealed at 441.5 K for 1 hour. The horizontal lines show R of the imaginary crystals melting from ζ_n to ζ = 0.

3. Conclusion

For iPS, PET, and iPP, the heat capacity jump at the glass transition was due to the discontinuous change of energy in quantum state of the photon holes between neighboring benzene rings, but methyl groups for iPP, followed by unfreezing of glass parts. For iPS and iPP, the homogeneous glasses free from ordered part / hole pairs with T_g= 240 K and 180 K were predicted, respectively. For iPP, the cohesive energy of methylene residues was subdivided into the transition enthalpies of glasses, ordered parts, and crystals, whereas for iPS, it agreed

with the difference between the transition enthalpies of glasses and ordered parts, but the transition enthalpy of glasses was larger than that of ordered parts. The photonic contribution of 60 % to the heat capacity jump at the glass transition found for PET meant that one photon was situated in the neighboring phenylene residues comprising ~60 % of the structural unit length and the residual jump of 40 % was brought by unfreezing of the ethylene glycol parts in a glass state. T_m^{∞}= 450 K for α form crystals of iPP could be the temperature of the quantum demand of hole energy at regular temperature intervals of 90 K. The shift of melting from α to γ form crystals by DSC measurements was done through the mediation of the formation and then disappearance of crystal / hole pairs. The interface parts formed in α and γ form crystals by annealing brought the excess energy of ~0.7 kJ/mol to the enthalpy of the ordered parts. This result was reflected clearly to the single crystal like image depicted on the basis of the crystal length distribution function.

4. A list of abbreviations (italic in Eqs.)

α : fraction of ordered part / hole pairs with C_v^{ph}

$1 - \alpha$: fraction of ordered part / hole pairs with C_p^{ph}

C_p : mean heat capacity per molar structural unit for ordered parts in ordered part / hole pairs

C_p^h : mean heat capacity per molar photon for holes in ordered part / hole pairs

C_p^{h*}: heat capacity per molar photon for holes in excited ordered part /hole pairs

C_p^{ph} : adiabatic molar heat capacity for photons

C_v^{ph} : constant volume molar heat capacity for photons

C_p^{flow} : heat capacity per molar structural unit for flow parts

C_p^r : heat capacity change per molar structural unit due to crystallization followed by melting

C_p^x: heat capacity per molar structural unit for ordered parts in excited ordered part /hole pairs

c : velocity of light

c* : cell length of c–axis

c_1 and c_2 : constants in WLF equation

dQ/dT : heat flow rate of DSC melting curves

δQ_m : heat change per molar structural unit per K

ΔC_p : heat capacity jump per molar photon at the glass transition

ΔC_p^{exp} : experimental heat capacity jump per molar structural unit at the glass transition

ΔC_p^x : relative component heat capacity per molar structural unit for excited ordered parts

Δh : additional heat per molar structural unit needed to melt all ordered parts

Δh^h : hole energy of crystal / hole pairs formed newly by recrystallization

δ : solubility parameter

E_a : activation energy

$F(\zeta)$: crystal length (ζ) distribution function

f : free energy per molar structural unit

f^{conf} : conformational free energy per molar structural unit

f_g^{conf} : conformational free energy per molar structural unit at T_g

f_x : free energy per molar structural unit for ordered parts

f_u : free energy per molar structural unit for crystals

ϕ : amorphous fraction

Γ : frequency of occurrence of the helix–coil transition

H_m^a : enthalpy per molar structural unit for the liquid at T_m^∞

H_c^a : enthalpy per molar structural unit for the super–cooled liquid at T_c

H_g^a : enthalpy per molar structural unit for the super–cooled liquid at T_g

H_g^c : enthalpy per molar structural unit for the crystal at T_g

h^h : hole energy per molar photon for holes in ordered part / hole pairs

h_0 : latent cohesive energy per molar structural unit

h_0^h : zero–point energy per molar photon, or energy unit per molar photon

h_u : heat of fusion per molar structural unit

h_x : enthalpy per molar structural unit for ordered parts

h_g : glass transition enthalpy per molar structural unit

h^{conf} : conformational enthalpy per molar structural unit

h_g^{conf} : conformational enthalpy per molar structural unit at T_g

h_x^{conf} : conformational enthalpy per molar structural unit for ordered parts

h^{int} : cohesive enthalpy per molar structural unit

h_g^{int} : cohesive enthalpy per molar structural unit at T_g

h_m^{int} : cohesive energy per molar structural unit for methylene residues

h : Plank constant

η : statistical weight

J_h : number of holes lost by T at the glass transition

φ_g : fraction of core free volume in glasses

λ and $1/\lambda$: wavelength and wave number

mol : molar structural unit

mol* : molar photon

μ : conversion coefficient of mol/m^3

N_A : Avogadro constant

N_c : number of structural units of crystals melted in the temperature range from T_b to T_e

n : number of structural units holding one photon potentially

n_ζ : number of crystal sequences with ζ

ν : frequency per second

P : pressure

P_c : probability that a sequence occupies the lattice sites of a crystalline sequence

Q : heat per molar structural unit corresponding to the total area of DSC endothermic curve

Q_m : heat per molar structural unit corresponding to the area of a DSC melting curve from T_b

R : gas constant

R_n : number of crystal sequences at the radius direction of an imaginary single crystal lamella depicted on the basis of $F(\zeta)$

s_u : entropy of fusion per molar structural unit

s_x : entropy per molar structural unit for ordered parts

s^{conf} : conformational entropy per molar structural unit

s_g^{conf} : conformational entropy per molar structural unit at T_g

σ_e : end surface free energy of a crystal per unit area

σ : statistical weight

T : temperature

T_g : glass transition temperature

T_m : melting temperature

T_m^∞ : equilibrium melting temperature

T_e and T* : end temperature of DSC melting peak curve

T_l : end temperature of the glass transition

T_c : onset temperature of DSC crystallization peak curve upon cooling

T_b : onset temperature of DSC melting peak curve upon heating

T_a : annealing temperature

T_p : DSC melting peak temperature

V : volume per molar structural unit

v_f : free volume per molar structural unit

v_0 : core free volume per molar structural unit

x : degree of polymerization

Z : conformational partition function for a chain

Z_0 : component conformational partition function for a chain regardless of temperature

Z_t : component conformational partition function for a chain depending on temperature

ζ : crystal length

ζ_p : crystal length at the maximum of $F(\zeta)$

ζ_n : crystal length at the minimum of ζ

ζ_x : crystal length at the maximum of ζ

Acknowledgements

The author would like to thank the late Professor em. B. Wunderlich of the University of Tennessee and Rensseler Polytechnic Institute for the long time encouragement.

Author details

Nobuyuki Tanaka*

Address all correspondence to: thermodyna_nt@kki.biglobe.ne.jp

Gunma University, Gunma, Japan

References

[1] T. G. Fox, P. J. Flory, J. Polym. Sci., 14, 315(1954).

[2] G. Natta, P. Corradini, D. Sianesi, D. Morero, J. Polym. Sci., 51, 527(1961).

[3] G. Gee, Polymer, 7, 177(1966).

[4] A. L. Renninger, D. R. Uhlmann, J. Polym. Sci., Phys., 16, 2237(1978).

[5] R. J. Roe, A. E. Tonelli, Macromolecules, 12, 878(1979).

[6] L. H. Judovits, R. C. Bopp, U. Gaur, B. Wunderlich, J. Polym. Sci., 24, 2725(1986).

[7] G. Brinke, L. Oudhuis, T. S. Ellis, Thermochimica Acta, 238, 75(1994).

[8] B. Wunderlich, "Thermal Analysis of Polymeric Materials", Springer, (2005).

[9] B. Wunderlich, J. Appl. Polym. Sci., 105, 49(2007).

[10] N. Tanaka, Y. Mastai Ed: "Advances in Crystallization Processes", InTech, p163(2012).

[11] N. Tanaka, Preprints of 45th Japanese Conference on Calorimetry and Thermal Analysis (Hachioji), p20(2009).

[12] N. Tanaka, Preprints of 46th Japanese Conference on Calorimetry and Thermal Analysis (Tsu), p27(2010).

[13] N. Tanaka, Preprints of 47th Japanese Conference on Calorimetry and Thermal Analysis (Kiryu), p27(2011).

[14] N. Tanaka, 62nd SPSJ Annual Meeting, Polymer Preprints (CD), Kyoto, 62, (2013).

[15] N. Tanaka, Preprints of 49th Japanese Conference on Calorimetry and Thermal Analysis (Narashino), p137(2013).

[16] N. Tanaka, 63th SPSJ Annual Meeting, Polymer Preprints (CD), Nagoya, 63, (2014).

[17] F. Zamponi, Nature Phys., 7, 99(2011).

[18] G. Biroli, Nature Phys., 10, 555(2014).

[19] N. Tanaka, Polymer, 33, 623(1992).

[20] L. H. Hill, "Introduction to Statistical Thermodynamics", Addison–Wisley, Massachusetts, p456(1960).

[21] T. McLeish, Physics Today, 61, No. 8, (2008).

[22] N. Tanaka, Thermochimica Acta, 374, 1(2001).

[23] N. Tanaka, Polymer, 49, 5353(2008).

[24] J. D. Ferry, "Viscoelastic Properties of Polymers", Reinhold, New York, (1961).

[25] M. Kobayashi, S. Hanafusa, T. Yoshioka, S. Koizumi, Japanese J. Polym. Sci. and Tech., 53, 575(1996).

[26] Spectroscopic Soc. of Japan, "Infrared and Raman Spectroscopy", Kodansha Sci., Tokyo, (2011).

[27] N. Tanaka, G. Wypych Ed: "Handbook of Solvents", ChemTech Publishing, Toronto, p253(2001).

[28] H. Burell, J. Brandrup, E. H. Immergut, "Polymer Handbook", Interscience, New York, (1966).

[29] C. W. Bunn, J. Polym. Sci., 16, 323(1955).

[30] H. Yoshida, Netsusokutei, 13(4), 191(1986).

[31] D. Y. Yoon, P. R. Sundararajan, P. J. Flory, Macromolecules, 8, 776(1975).

[32] G. Allegra Ed: "Interfaces and mesophases in polymer crystallization 2", Berlin, Springer, p288(2005).

[33] J. Stokr, B. Schneider, D. Doskocilova, J. Lovy, P. Sedlacek, Polymer, 23, 714(1982).

[34] B. Wunderlich, ATHAS databank (1992 Recommended Data).

[35] N. Tanaka, 56th SPSJ Annual Meeting, Polymer Preprints (CD), Nagoya, 56, (2006).

[36] P. J. Flory, J. E. Mark, A. Abe, J. Am. Chem. Soc., 88, 639(1966).

[37] A. Nakajima, M. Hosono, "Molecular Properties of Polymers", Kagakudojin, (1969).

[38] N. Tanaka, Polymer, 34, 4941(1993).

[39] N. Tanaka, 58th SPSJ Annual Meeting, Polymer Preprints (CD), Kobe, 58, (2009).

[40] P. J. Flory, J. Chem. Phys., 17, 223(1949).

[41] J. P. Luongo, J. Appl. Polym. Sci., 3, 302(1960).

[42] J. X. Li, W. L. Cheung, D. Jia, Polymer, 40, 1219(1999).

[43] N. Tanaka, Proceedings of the 5th Italian Conference on Chemical and Process Engineering, Florence, 949(2001).

[44] N. Tanaka, H. Fujii, J. Macromol. Sci., B42, 621(2003).

[45] N. Tanaka, Gunma University, Japanese Patent 4228080.